Autonomous Navigation For Moon Missions: A Realistic Performance Assessment, Considering Earth GNSS Signals And LCNS Constellation

MARCO MANGIALARDO, MARIA MANZANO JURADO, DAVID HAGAN, PIETRO GIORDANO, PAOLO ZOCCARATO, JAVIER VENTURA-TRAVESET

IVÁN CORRAL

Index

Objective

Lunar exploration is going to have a central role in the future of space industry. The use of weak-GNSS signals to navigate spacecraft in cislunar space has been investigated in several publications, bringing the advantage of being less expensive and based on already existing infrastructure, allowing to improve **accuracy, robustness and autonomy** but this concept has some limitations (users on the far side of the Moon)

This paper's goal is to perform a representative end-to-end assessment of what are realistic navigation performance achievable by an autonomous GNSS navigation system for two Moon mission scenarios: Lunar Pathfinder and Low Lunar Frozen Orbit (LLFO). In addition, preliminary performances using a potential LCNS constellation are assessed, together with Earth GNSS or standalone.

Introduction

The current navigation approach for Moon missions relies on a combination of multiple on-board sensors and radiometric measurements with **Earth ground stations**. The employment of such measurements, allowed to achieve orbit determination with **accuracies in the order of tens of meters**. However, these techniques rely on ground operations, increasing the cost of such missions. Moreover, the ground resources might not be enough to service all of the potential future missions to the Moon.

GNSS signals coming from Earth's constellations, can be received and acquired at Moon distance, as proven in some papers with GPS signals.

Introduction

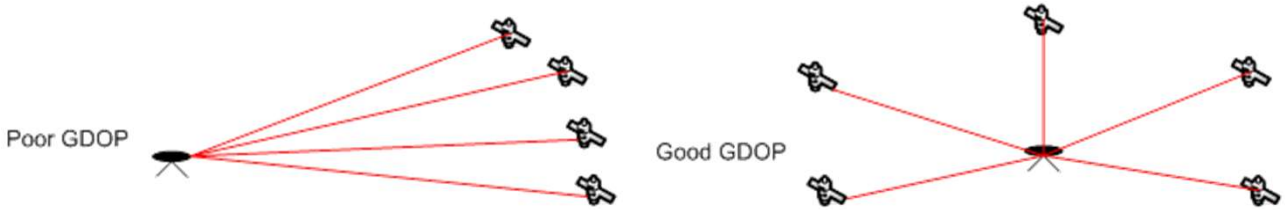

There are some significant limitations present:

- far-side landing and operations could not utilize Earth GNSS signals, orbiting satellites at low altitudes would experience continuous occultation.

Space agencies proposed dedicated systems to **provide navigation and communication services for lunar missions**.

- NASA recently introduced a concept called Cislunar Autonomous Positioning System (**CAPS**), with the objective of providing autonomous navigation services in cislunar space. CAPS would use inter-satellite link range and range-rate measurements between cooperating satellites to provide absolute inertial and relative positioning.
- The European Space Agency Lunar Communication and Navigation Service (**LCNS**) is aimed to provide communication and navigation services for a wide range of institutional and commercial Moon missions. The idea is to use the most recent GNSS satellite technology to implement a one-way broadcast solution, while keeping the possibility to supply an additional two-way navigation service. The current idea is to have **5 satellites**, orbiting in Elliptical Lunar Frozen Orbits (ELFOs), distributed in 3 different planes.

Currently only three out of the five LCNS satellites are utilized, in order to target the horizontal positioning of a lunar rover in the proximity of the South Pole. A formal horizontal **precision in the order of tens of meters** is achieved when the horizontal dilution of precision is around or below 10 and three LCNS satellites are in view [2]. In another studio, the estimation performed is **kinematic**, which implies that the navigation solution is competitive only when good visibility and DOP are achievable and the navigation error quickly diverges from the best achievable value of around **30 meters** [3].

Proof of Concept Overview

The Proof of Concept (PoC) simulator is an end-to-end software tool whose objective is to assess the navigation performance for different lunar mission orbiting scenarios. The PoC simulator can generate scenarios considering both **Earth GNSS and LCNS satellites**, either simultaneously or one at the time. The simulator consists of three modules

- **Scenario Generator Module** (SGM) – In charge of **simulating the scene**, with all of the features contributing to Moon-GNSS based navigation. The main outputs of this module are user reference trajectories, satellite visibility scheme, signal received power, measurements for ranges and Doppler shifts.
- **GNSS Receiver Module** (GRM) – Its objective is to simulate the behaviour of a high-sensitivity **GNSS receiver**, capable of acquiring and tracking both Earth GNSS weak signals and LCNS signals. The main outputs are pseudorange and Doppler measurements.
- **Navigation Filter Module** (NFM) – This module implements purely **GNSS navigation filters** and assess navigation performance for each scenario

Scenarios Description

The objective of this work is to determine the performance of autonomous GNSS-based navigation for Moon missions and evaluate the improvement introduced by lunar augmentation system. In order to do this, two key orbiter scenarios were identified:

- **Lunar Pathfinder Orbit**: Due launch by the end of 2023, this mission is going to test for the first time a high sensitivity LCNS receiver [4]. Performance as good as **50 meters RMS** positioning error can be expected, even using only Earth GNSS satellites.
- **Low Lunar Frozen Orbit** (LLFO): Circular orbit close to the Moon surface are normally employed as parking orbits before descending (or after ascending) to the lunar surface. Compared to the Lunar Pathfinder, this scenario is more challenging in terms of navigation, because of the faster dynamics, continuous Moon occultation and proximity to the surface.

Scenarios Description

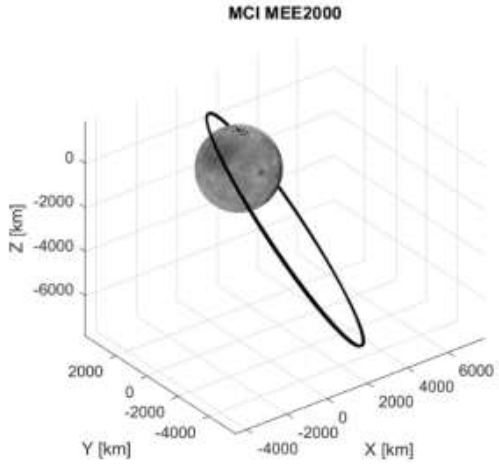

Lunar Pathfinder in MCI 2000

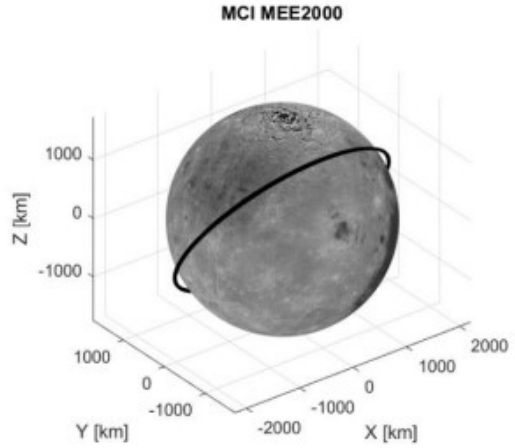

Low Lunar Frozen Orbit in MCI2000

Scenario	Orbits Definition					
	SMA [km]	*e [-]*	*i [deg]*	*RAAN [deg]*	*Arg. Per. [deg]*	θ_0 *[deg]*
Lunar Pathfinder	5736	0.61	57.8	61.5	90	0
LLFO	1838	0	55.3	0	0	0

Scenario Generator Module

Within the SGM, all of the features contributing to Moon-GNSS based navigation are simulated. Spacecraft dynamics and GNSS and LCNS trajectories are computed, in order to assess the relative geometry between them.

Effects such as Earth and Moon signal occultation, direction of the different GNSS signals, visibility and power link budget (using Earth GNSS 3D emitters antenna gain patterns) are taken into account with advanced models, in order to simulate a scene that is as representative as possible of potential Moon missions.

Particular attention was placed on the generation of broadcast GNSS navigation message, with the aim of obtaining realistic errors on GNSS orbits and clocks

Scenario Generator Module

For the orbiter scenarios, the **spacecraft reference trajectory** considers a point mass dynamics in which the following effects are considered: Earth central gravity, Moon central gravity, Sun central gravity, Earth harmonics (to a degree of 20), Moon harmonics (to a degree of 50), and solar radiation pressure (reflectivity coefficient of 1.2 and SC dimensions 1.35x1.35x0.9 m). Earth, Moon and Sun positions are computed using JPL Ephemeris.

The SGM includes a highly representative **reference clock model**, For the receiver clock, the parameters considered correspond to an OCXO clock, therefore the values used for the Allan Deviation at 10 MHz are: 3e-12 @ 3secs and 1e-11 @ 20 minutes. To compute GPS and Galileo reference clocks, the same clock model is used with different parameters. In particular, the following clock model parameters can be simulated: GPS Block III Rubidium Clocks and Galileo Passive Hydrogen Maser Clocks.

Concerning the **receiver antenna**, two options were considered:

- **high gain antenna** to capture low power signal coming from **Earth GNSS satellites**. Its characteristics are in line with the preliminary specifications of the antenna that will fly in the Lunar Pathfinder experiment" [3], which has a 15\11.5 dB peak for L1\L5 bands and a field of view of roughly 20°
- **low gain hemispherical antenna** to acquire **LCNS signal**.

The PoC simulator featured the possibility of using both antennas simultaneously, in order to acquire Earth GNSS and LCNS signal at the same time. For the orbiter scenarios, it is assumed that an Earth pointing mechanism for the high-gain antenna is possible, which is a reasonable assumption for the Lunar Pathfinder mission, for which a pointing mechanism is planned as part of the experiment. For the LLFO case it is less probable that an Earth pointing mechanism will be included, however the results presented contemplate also this possibility.

Scenario Generator Module

One of the main aspects affecting navigation performance is the **accuracy** obtainable for GNSS satellites positions, velocities and clocks, which, for autonomous navigation, is driven by the Earth GNSS broadcast **ephemeris error**. In the case of Earth GNSS weak signals, the capability of demodulating the navigation message is also fundamental and must be taken into account. An assessment of the error degradation with respect to the broadcast message Age-Of-Data (AOD) was done during this study, to carefully represent cases in which non-updated broadcast ephemeris are used for longer periods of time. The final choice was to use broadcast messages not older than 2 hours.

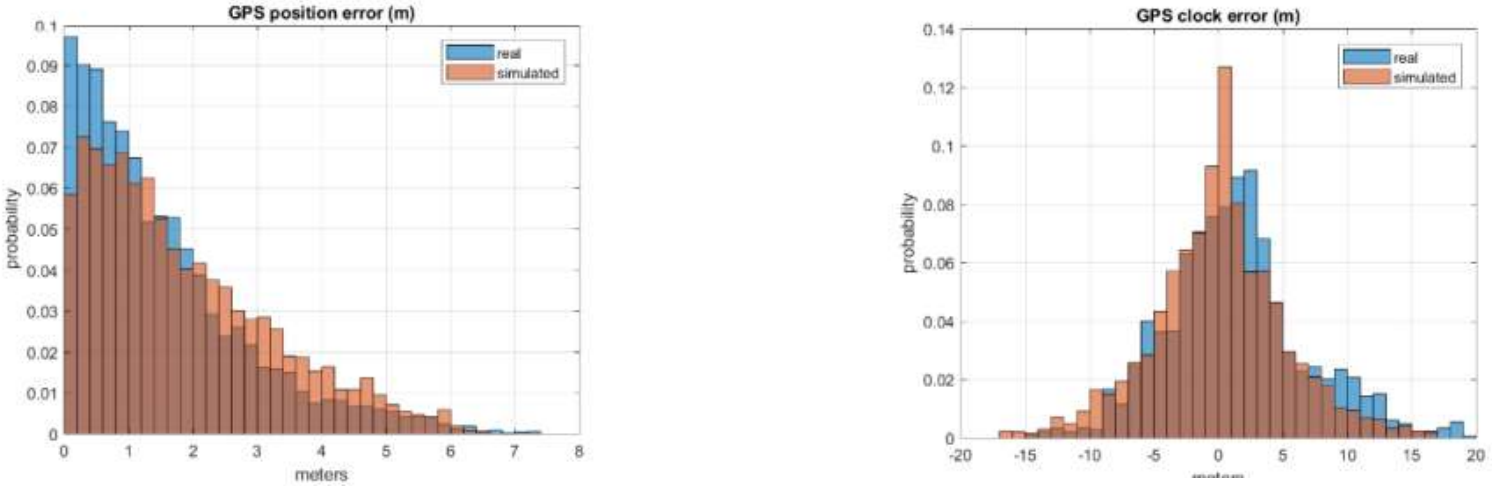

GPS position and clock errors of Broadcast Ephemeris (within 2 hours). Errors obtained using real BRDC data (blue) and simulated BRDC data (orange) are compared.

Scenario Generator Module

Another key feature of the present work is the usage of three-dimensional Earth GNSS **antenna gain patterns**. Most of Earth GNSS signal reaching the Moon comes from the secondary lobes.

Two different “layers” of received power can be observed:

- The first one, on the top (from 37 to 25 dBHz) is less dense and it comes from the **main lobes** of the GNSS satellite antennas.
- The bottom layer (from 25 dBHz below) contains the signal coming from the **side lobes** of the GNSS satellites and it is denser.

To realistically assess navigation performance using Earth GNSS signal, the secondary lobes must be modeled carefully and a high-sensitivity GNSS receiver needs to acquire a sufficient number of signals, including the ones coming from the side lobes.

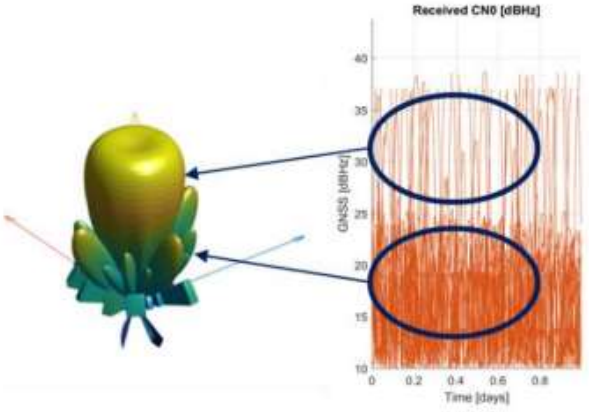

Example of received C/N0 from Earth GNSS satellites, for a Moon orbiter

Scenario Generator Module

The **GPS and Galileo constellations** are modelled considering a potential future scenario in 2025, which assumes 24 Galileo satellites and 30 GPS satellites. The final feature simulated in the SGM is LCNS augmentation.

The **lunar GNSS architecture** considered in this work implements 5 satellites, orbiting in three different Elliptical Lunar Frozen Orbits (ELFO). These orbits were selected for their coverage of the Moon's South Pole and for their stability over time, requiring low orbit-keeping cost. The 3 different ELFO planes are separated by 120° and the orbital parameters. The LCNS satellites are spread by means of three different planes and different initial true anomalies in order to maximize the Geometric Dilution Of Precision (GDOP) on the Moon surface

N	Orbital Parameters					
	SMA [km]	*e [-]*	*i [deg]*	*RAAN [deg]*	*Arg. Per. [deg]*	*Initial θ [deg]*
1	9750.5	0.7	63.2	0	90	0
2	9750.5	0.7	63.2	120	90	164
3	9750.5	0.7	63.2	240	90	196
4	9750.5	0.7	63.2	120	90	245
5	9750.5	0.7	63.2	240	90	184

LCNS Orbital Parameters

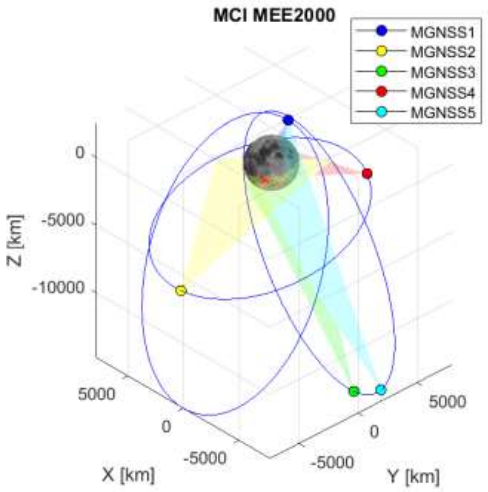

LCNS satellites

Scenario Generator Module

LCNS space segment, including **LCNS satellites navigation** payload is yet to be defined precisely, nevertheless some reasonable assumptions can be made. As compared to Earth GNSS satellites, LCNS satellites in this configuration will have a **smaller maximum surface distance**: 14840 km against 20200 km for GPS and 23222 km for Galileo. This allows to **reduce** the Emitted Isotropic Radiated Power (**EIRP**) of the LCNS emitters with respect to Earth GNSS values, therefore reducing size, weight and power of the navigation payload.

EIRP=12 dBW, with a gain pattern Field Of View (FOV) of 40 degrees (+/- 20degree from boresight).

With regards to the carrier frequency, the **S-band** is the preferred candidate as it would allow to re-use many of the Earth GNSS technology, while avoiding interference with them when weak GNSS signals are used in cis-lunar space. Signals coming from Earth GNSS satellites might be indeed used together with LCNS, therefore averting interference is desirable.

fc=2.495 GHz

Similar to Earth GNSS, **LCNS ephemeris errors** represent the residual error experienced at user level after the application of the LCNS navigation message.

$$\mathcal{E}_{ephemeris} = 25 \text{ m}$$

at 95th percentile for the projection of the 4 components (3 for position and 1 for time) on the user light of sight, at maximum AOD

GNSS Receiver Module

The GRM oversees generating pseudorange, velocity and carrier phase measurements, representing the behaviour of a lunar-tailored designed receiver. This block implements the Observable Generator Module (OGM), whose main objective is to generate **pseudoranges and Doppler measurements**, with the appropriate performance. The performance is determined by the type of received satellite signals and their corresponding parameters.

The module includes:

- near-far processing: interference between two signals with a large difference in received signal powers
- acquisition observable generation: in terms of acquisition probability and estimation accuracy
- a full tracking module encompassing a Phase-Locked Loop (PLL), Frequency-Locked Loop (FLL) and an FLL-assisted PLL for carrier phase tracking and a Delay-Locked Loop (DLL) for code tracking
- the logic for generating the measurements, based on acquisition\tracking results and status

GNSS Receiver Module [13]

The feasibility of demodulating the broadcast navigation message is also assessed as a function of the **received C/N0**. Once tracking is declared successful, the GRM performs an analysis on whether the navigation message (ephemeris and almanacs) can be successfully decoded.

$$\frac{C}{N_0} = P_{r_x} + {}^{g}/_{T} - k \qquad T_{sys} = T_0 \times (10^{\frac{NF}{10}} - 1) \qquad P_{r_x} = EIRP(\beta) - FSPL \qquad FSPL = 20\log_{10}\left(\frac{4\pi \times d \times f_c}{c}\right)$$

k= -228.6 dBW/K/Hz (Boltzmann constant) ${}^{g}/_{T}$ is the gain-to-noise-temperature ratio, where g is the antenna gain in dBi in the receiving direction

Time	Frequency band (MHz)	GNSS Satellite	Off-boresight angle β (deg)	EIRP in β (dBW)	Distance (km)	FSPL (dB)
09-Nov-2025 09:55:59.749	E5a = 1176.45	Galileo SVID 01	65	3.744	381643.1	205.4924
Rcvd. Iso. Power (dBW)	**Receiving off-boresight direction Θ (deg)**	**Receiver Antenna Gain in Θ (dBi)**		**T_{eq} (K)**	**g/T (dB/K)**	**C/N_0 (dB-Hz)**
-201.75	4.156	12.6633		282.619	-11.849	15.00001

Detailed Link Budget between Galileo SVID 01 and DSG

GNSS Receiver Module [24]

The data demodulation thresholds were computed by intersecting the CED error rate curves obtained by Monte Carlo simulations with a **threshold value equal to 10^{-2}**. This means that, if during the considered simulation time the received signal has an average C/N0 equal to or bigger than the computed threshold, the **CED will be correctly decoded at least 99 times out of 100**

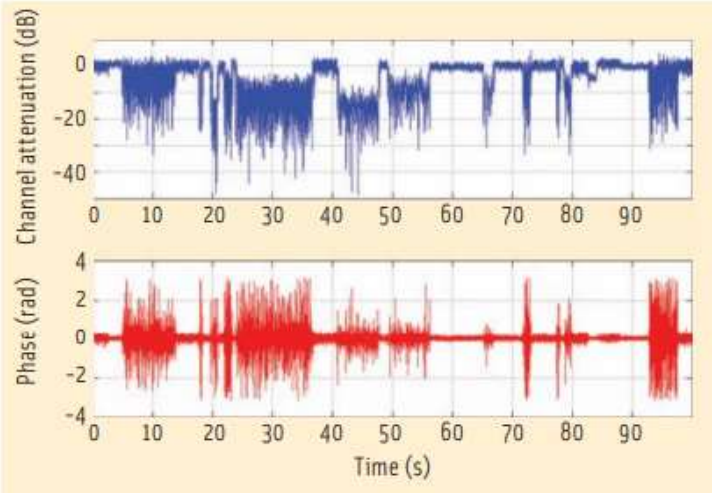

Amplitude and phase of the LMS channel coefficients used for the simulations (first 100 seconds of realization)

	Demodulation threshold @ CED error rate = 10^{-2}					
	GPS				Galileo	
	L1 C/A	L2C	L5	L1C	E1 OS/E5b	E5a
Message	*NAV*	*CNAV*	*CNAV*	*CNAV-2*	*I/NAV*	*F/NAV*
Total required C/N_0 [dBHz]	26.5	23.1	26.1	24.5	27.7	20.7

TABLE 7. Data demodulation performance of GPS and Galileo signals in AWGN channel

	Demodulation threshold @ CED error rate = 10^{-2}					
	GPS				Galileo	
	L1 C/A	L2C	L5	L1C	E1 OS/E5b	E5a
Message	*NAV*	*CNAV*	*CNAV*	*CNAV-2*	*I/NAV*	*F/NAV*
Total required C/N_0 [dBHz]	60.2	38.5	42.9	33.8	42.8	32.7

TABLE 8. Data demodulation performance of GPS and Galileo signals in LMS channel

GNSS Receiver Module

This is based on input **C/N0** and **tracking status of each satellite**, and on the **time** required to decode ephemeris and almanac data, which are independent from one another. For each case and for each PRN, it is analyzed whether the navigation message can be decoded or not.

Signal	C/N0 threshold [dBHz]	Time required to decode ephemeris [s]	Ephemeris validity [h]	Time required to decode almanacs [s]	Almanacs validity [d]
GPS L1 C/A	26.5	48	4	1200	12
GPS L1c	24.5	48		1200	
GPS L5	26.1	24		600	
Galileo L1	27.7	30		720	
Galileo L5	20.7	50		600	

Time required to decode ephemeris message (FNAV assumed)

Other effects are also considered in the simulation, such as the **local multipath in the GNSS measurements**, simulated as a function of the elevation of the arriving signal.

GRM can provide measurements for a potential future LCNS constellation, based on the assumption that the user can configure the following parameters: **LCNS carrier frequency** (Hz), **LCNS modulation type** (based on existing GPS and Galileo modes, in terms of bandwidth (Hz), code period (ms), chip rate / chip period (seconds)).

Navigation Filter Module

The NFM is the last part of the PoC simulator and it is in charge of **obtaining the navigation solution**. Considering the characteristics of the considered scenarios, an **Extended Kalman Filter** was considered to be the most suitable option.

It combined an on-board dynamic model with the measurements to obtain the navigation solution. The EKF represents the standard technique in the field of linear or linearized state estimation and they are widely applied in GNSS-based navigation systems.

Navigation Filter Module
Architecture Trade-Off

GNSS EKF architecture using PVT update

The satellite state PVT is computed using the GNSS measurements in a **Single Point Positioning** and then uses this computed PVT to fit the dynamic model in the filter measurement update.

This option is simpler but requires at least **four GNSS available satellites** to perform an update. When four GNSS satellites are not available the state vector is propagated using the on-board satellite **dynamic model** but no update is performed, leading to a **degradation of the solution** because of the integration of the mismodelling and omitting errors

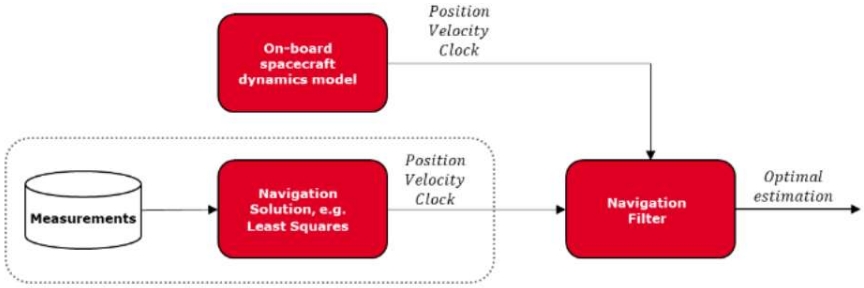

GNSS EKF architecture using measurements update

Pseudorange and Doppler measurements are used as inputs and it **can be used even when only one single GNSS satellite is visible**. Considering that the number of signals reaching the Spacecraft are very low, and that the received power from Earth GNSS satellites at Moon distance is weak, the probability of receiving, acquiring and tracking a GNSS signal is low and, therefore, a small number of measurements will be normally available in the navigation filter.

Here the filter measurement update is performed even when less than 4 GNSS measurements are available.

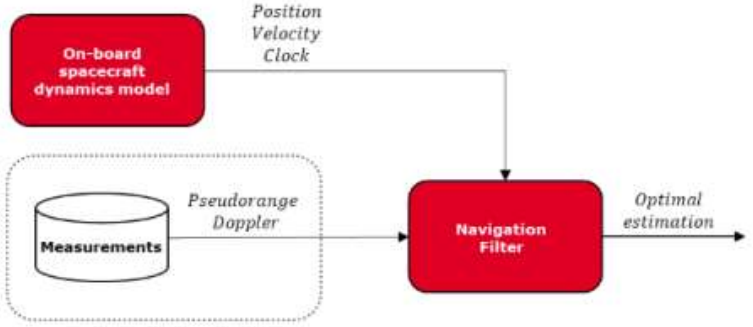

The impact that the first option would have on navigation performance was considered unacceptable, therefore the **second option architecture was chosen.**

Navigation Filter Module
Dynamic model

Concerning the state and the on-board dynamics model, the navigation filter algorithm features 9 elements, namely 3 elements for the **spacecraft position** p_r , 3 for the **spacecraft velocity** v_r, a **receiver clock bias** b_r , a **drift** d_r and an **aging** a_r

$$\boldsymbol{x} = [\boldsymbol{p}_r^T\ \boldsymbol{v}_r^T\ b_r\ d_r\ a_r]^T$$

As Earth GNSS signals are weak in Moon's proximity, the number of measurements available in the navigation filter is lower than in Earth applications. For this reason, using a precise on-board software dynamics model is a key aspect of such navigation technique, especially when considering Earth GNSS only.

The on-board dynamics utilizes simplified models of the main accelerations acting on the high-fidelity reference trajectory, thus simulating the discrepancy between on-board model and real dynamics:

- Earth central gravity
- Moon central gravity
- Sun central gravity
- Moon harmonics to a degree and order of 10.

By propagating the on-board dynamic model for 2 days without using the measurements, the error obtained (with respect to the **reference trajectory**) is in the order of 2 km for the Lunar Pathfinder and 12 km for the Low Lunar Orbit. The same dynamic model results less accurate the closer the trajectory is to the Moon's surface, because of the growing effect of the lunar harmonics

Scenario	Process Noise ($\sqrt{Q}$)	
	Position [m]	*Velocity [m/s]*
Lunar Pathfinder	1e-5	3.16e-4
LLFO	3.16e-4	1.14e-2

Process Noise used in the EKF for each orbiter scenario

Navigation Filter Module
Dynamic model

Concerning the on-board **clock bias model**, a second order polynomial model is used. The state discrete propagation utilizes a Runge-Kutta 4 fixed-step:

$$\dot{\boldsymbol{p}}_r = \boldsymbol{v}_r$$

$$\dot{\boldsymbol{v}}_r = \boldsymbol{a}_{Moon} + \boldsymbol{a}_{Earth} + \boldsymbol{a}_{Sun} + \boldsymbol{a}_{NonSphMoon_{10,10}}$$

The clock is interpolated as:

$$\dot{b}_r = d_r$$

$$\dot{d}_r = a_r$$

$$\dot{a}_r = 0$$

Navigation Filter Module
Measurements and their covariance

Both pseudoranges and Doppler measurements are used in the navigation filter, considering 12 channels each, for a maximum 24 measurements for each navigation step. **Measurement covariance is computed in the navigation filter as a function of the received power:**

$$\sigma_{Meas} = SF * \sqrt{\left(\frac{1}{10}\right)^{\frac{CN_0}{10}}}$$

SF is a scale factor, interpreted as a tuning parameter, which changes depending on the scenario, the band considered, the GNSS receiver acquisition and tracking process, the expected $C/N0$ and depending on the measurement being pseudorange or Doppler

Navigation Filter Module
Fundamental steps

A Kalman Filter is composed by 3 steps:

The **a-priori state** update

It takes as an input the previous optimal state estimation (x_k-1) and propagates it through the previously described on-board models

$$\hat{\boldsymbol{x}}_{k|k-1} = f(\hat{\boldsymbol{x}}_{k-1|k-1})$$

$$\boldsymbol{P}_{k|k-1} = \boldsymbol{F}_k \boldsymbol{P}_{k|k-1} \boldsymbol{F}_k^T + \boldsymbol{Q}_k$$

$$\boldsymbol{F}_k = \left.\frac{\partial f}{\partial \boldsymbol{x}}\right|_{\hat{\boldsymbol{x}}_{k-1|k-1}}$$

$\hat{\boldsymbol{x}}_{\boldsymbol{k}\,|\,\boldsymbol{k-1}}$ identifies an estimate of $\boldsymbol{x}$ at the time k, including all the observations up to time $k - 1$.

$\boldsymbol{P}$ is the state covariance matrix

$\boldsymbol{F}$ is the state transition

$\boldsymbol{Q}_{\boldsymbol{k}}$ is the covariance of the process noise

The **second step**: the a-priori measurement update

It depends on the propagated state and the best estimation of the GNSS Position, Velocity and Time (PVT), through a measurements model.

$$\boldsymbol{z}_k = h(\boldsymbol{x}_k) + \boldsymbol{v}_k$$

$$\boldsymbol{H}_k = \left.\frac{\partial h}{\partial \boldsymbol{x}}\right|_{\hat{\boldsymbol{x}}_{k|k-1}}$$

$$\hat{\boldsymbol{z}}_{PR,k|k-1} = \left\|\hat{\boldsymbol{p}}_{k|k-1} - \boldsymbol{p}_{GNSS}\right\| + \boldsymbol{b}_r$$

$$\hat{\boldsymbol{z}}_{Dop,k|k-1} = \left\|\hat{\boldsymbol{v}}_{k|k-1} - \boldsymbol{v}_{GNSS}\right\| + \boldsymbol{d}_r$$

$\boldsymbol{z}k$ are the measurements

$\boldsymbol{H}k$ is the observation matrix

$\boldsymbol{v}k$ is the observation noise, whose covariance is $\boldsymbol{R}k$

$\tilde{\boldsymbol{y}}_{\boldsymbol{k}}$ is the measurement residual

$$\tilde{\boldsymbol{y}}_k = \boldsymbol{z}_k - h(\hat{\boldsymbol{x}}_{k|k-1})$$

$$\boldsymbol{S}_k = \boldsymbol{H}_k \boldsymbol{P}_{k|k-1} \boldsymbol{H}_k^T + \boldsymbol{R}_k$$

$\boldsymbol{s}_{\boldsymbol{k}}$ is the residual covariance

The **third step**

It uses the near optimal Kalman gain to update the state and covariance estimate

$$\boldsymbol{K}_k = \boldsymbol{P}_{k|k-1} \boldsymbol{H}_k^T \boldsymbol{S}_k^{-1}$$

$$\hat{\boldsymbol{x}}_{k|k} = \hat{\boldsymbol{x}}_{k|k-1} + \boldsymbol{K}_k \tilde{\boldsymbol{y}}_k$$

$$\boldsymbol{P}_{k|k} = (\boldsymbol{I}_{9,9} - \boldsymbol{K}_k \boldsymbol{H}_k) \boldsymbol{P}_{k|k-1}$$

Navigation Filter Module
Fundamental steps

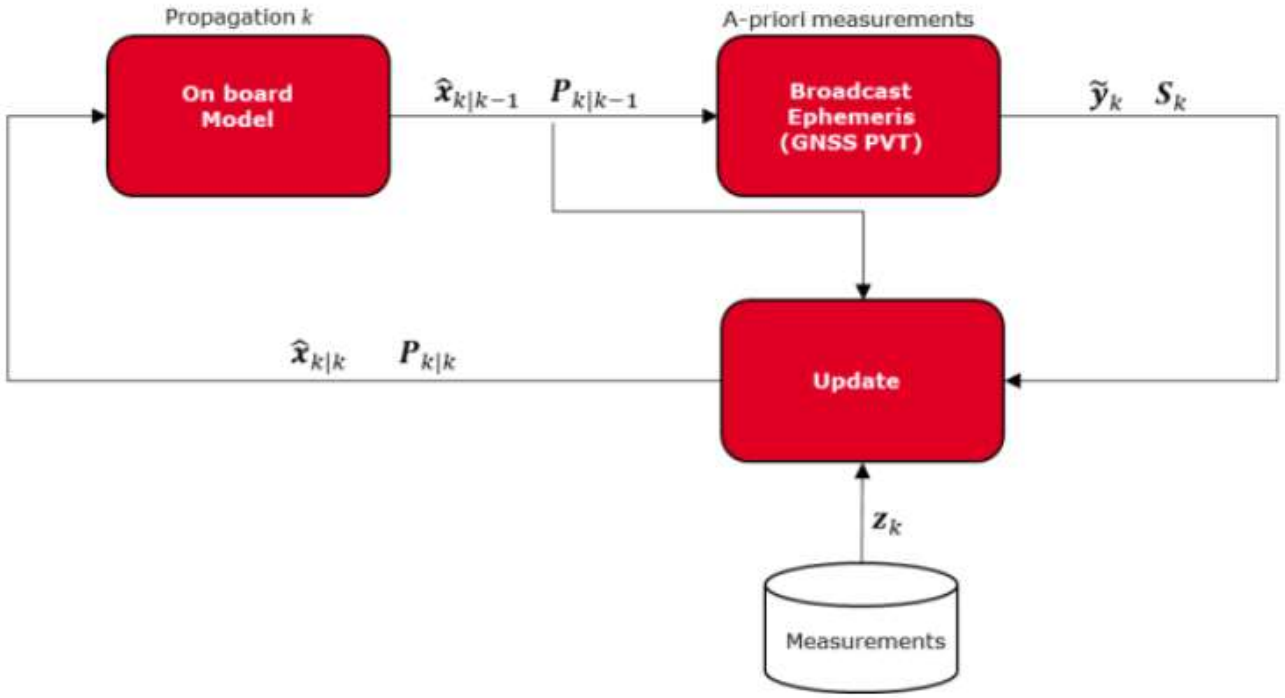

GNSS EKF high level scheme

Results

The objective of the simulations is to assess the navigation performance possible with purely Earth or LCNS signal and, evaluate the improvement introduced by the combination of the two. The test campaign considered two different scenarios, Lunar Pathfinder and Low Lunar Frozen Orbit.

- **Lunar Pathfinder**: Earth GNSS only, Earth GNSS plus LCNS combined.

  Such orbit is out of the LCNS service volume, so the improvement using LCNS is limited. Lunar Pathfinder mission will include an Earth pointing antenna, being a perfect candidate to evaluate navigation performance.

- **Low Lunar Frozen Orbit**: Earth GNSS only, LCNS only, Earth GNSS plus LCNS combined.

  Acceptable navigation performance are achievable with Earth GNSS alone, however, including LCNS improves drastically navigation performance.

Results

Simulation Main Parameters

Simulation Step Size	60 seconds	Navigation Step Size	60 seconds
Band Considered	GPS L1CA, Galileo E1 (1575.46e6 Hz), LCNS S-band (2.495 GHz)	Rx Antenna 1 (aims for Earth GNSS)	15 dBi peak (L1/E1)
Rx Antenna 1 Orientation	Earth Pointing (Perfect)	Rx Antenna 2 (aims for LCNS)	Low Gain Emispherical Antenna, 4 dBi peak
Rx Antenna 2 Orientation	Moon Zenith	Acquisition/Tracking Sensitivity	15/15 dBHz
Acquisition/Tracking Sensitivity LCNS	25/25 dBHz	Rx Clock Parameters	OCXO, Frequency 10 MHz, Frequency stability 25 ppb
Broadcast Ephemeris use	Maximum age 6 hours	Earth GNSS Configuration	30 GPS and 24 Galileo (L1CA/E1)
GPS 3D Gain	[4] Gives L1 gain patterns. For L5, the patterns are the same, with different EIRP	Galileo 3D Gain	(Confidential, provided by ESA)
LCNS Configuration	5 Satellites, 3 Planes	LCNS Antenna	12 dBW EIRP, 40 degree Field of View
Link Budget Noise Factor Loss	-1.036 dB (Active antenna)	Link Budget A/D Conversion Loss	-0.16 dB (3 bits quantization)
Link Budget Eq Syst Noise Temp	190 K		

Results [4]
GPS 3D Gain

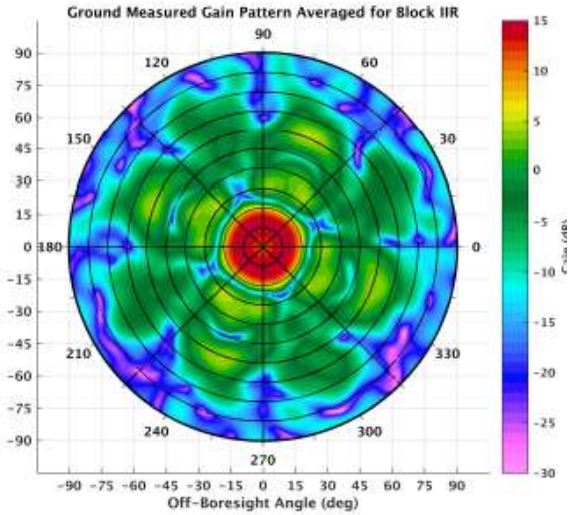

Block IIR ground measured antenna pattern

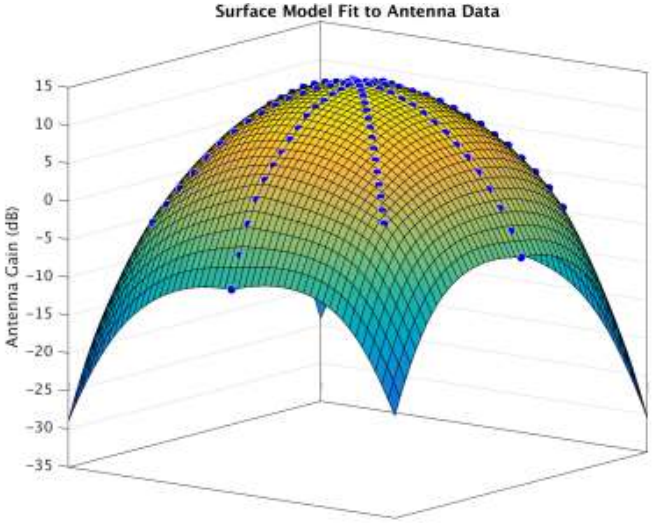

Smooth surface fitted to sparse receive antenna gain data.

Results
Received signals

The statistics for Earth GNSS satellites, include mean and standard deviation values for the **received power**, the number of **GNSS satellites above a threshold** of 15 dB/Hz and the number of **GNSS satellites available** in the navigation filter. The value for these two latter parameters can change significantly because the first one doesn't take into account the receiver module; therefore acquisition\tracking of the signal and demodulation of the navigation message are not considered.

Concerning LCNS statistics, the parameters described are the **received power** and the number of **LCNS satellites available** in the navigation filter. Contrarily to Earth GNSS, in this case the **received power is higher**, therefore almost every LCNS satellite in sight is available in the navigation filter

Scenario	Parameter				
	EGNSS CN_0, mean and STD [dBHz]	*Num of EGNSS over 15 dBHz, mean and STD*	*Num of EGNSS in NFM, mean and STD*	*LCNS CN_0, mean and STD [dBHz]*	*Num of LCNS available, mean and STD*
Lunar Pathfinder	21.76 5.07	11.38 2.27	2.63 1.38	32.05 4.09	2.48 1.52
Low Lunar Frozen Orbit	21.18 4.76	9.68 2.24	2.00 1.10	37.19 4.36	2.70 1.70

Received signal statistics for the two different scenario

Results
Received signals

It can be observed as the **signal received from Earth GNSS satellites is quite consistent** for the two scenarios (always assuming an Earth pointing high gain antenna).

The mean of the signals is around **21** $dBHz$ with a **standard deviation of roughly 5** dB, for L1CA/E1. This highlights the importance of implementing a tailor designed **high sensitivity GNSS receiver**, in order to acquire a sufficient number of GNSS satellites to be used in the navigation filter.

The results concerning **LCNS satellites** underline how the scenario included within the service volume of the constellation (LLFO) experiences **better visibility and received power**, which will be reflected in the navigation performance. Despite being within the service volume of the constellation, the LLFO coverage is not as good as it is for the South Pole's surface (LCNS constellation is designed to service the lunar South Pole).

The Lunar Pathfinder, despite being outside of the LCNS service volume, experiences decent visibility. Being an elliptical polar orbit, the spacecraft is located most of the time between the Moon and the LCNS satellites, above the lunar Southern Hemisphere, where the visibility is optimal.

Scenario	Pseudorange Noise Average STD		
	GPS [m]	*GAL [m]*	*LCNS [m]*
Lunar Pathfinder	2.98	2.94	1.29
Low Lunar Frozen Orbit	3.19	3.02	1.13

Pseudorange measurement's noise average standard deviations

Results

Navigation Performance: Lunar Pathfinder

Navigation performance, in the case of Lunar Pathfinder orbiter, is obtained using the **Extended Kalman Filter**.

This scenario seems to be particularly suitable to perform even a purely Earth GNSS based navigation, considering that decent visibility is achievable with the Earth. This orbit suffers from **Moon occultation**, but it is quite modest and **doesn't affect navigation performance** if an accurate on-board dynamics model is implemented in the filter.

It can be observed as the introduction of the LCNS augmentation has a relatively minor impact on the already excellent navigation performance obtained using Earth GNSS satellites only.

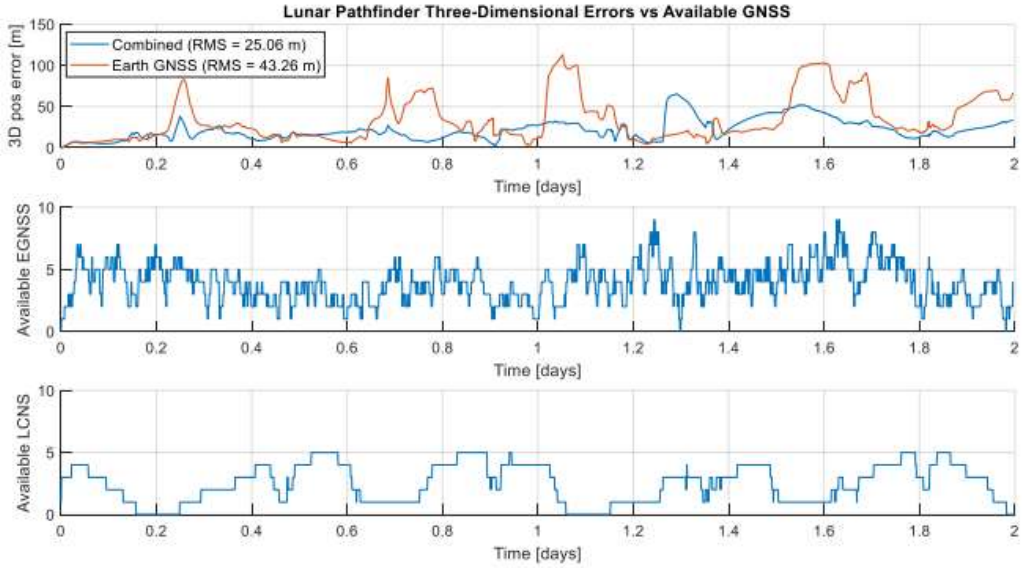

Lunar Pathfinder Navigation Performance for different cases. LCNS and Earth GNSS combined (blue), Earth GNSS only (orange).

Results

Navigation Performance: Low Lunar Frozen Orbit

Low Lunar orbits don't return good navigation performance when Earth-GNSS satellites are employed alone. The number of Earth GNSS satellites available in the navigation filter is much lower, compared to the Lunar Pathfinder. In addition, the same onboard dynamic model will result to be less accurate in this case, because of the vicinity to the Moon's surface.

The advantage introduced by LCNS constellation is huge.
An excellent navigation performance is obtained when using only **LCNS satellites: 83.34 meters in terms of root mean square error**.

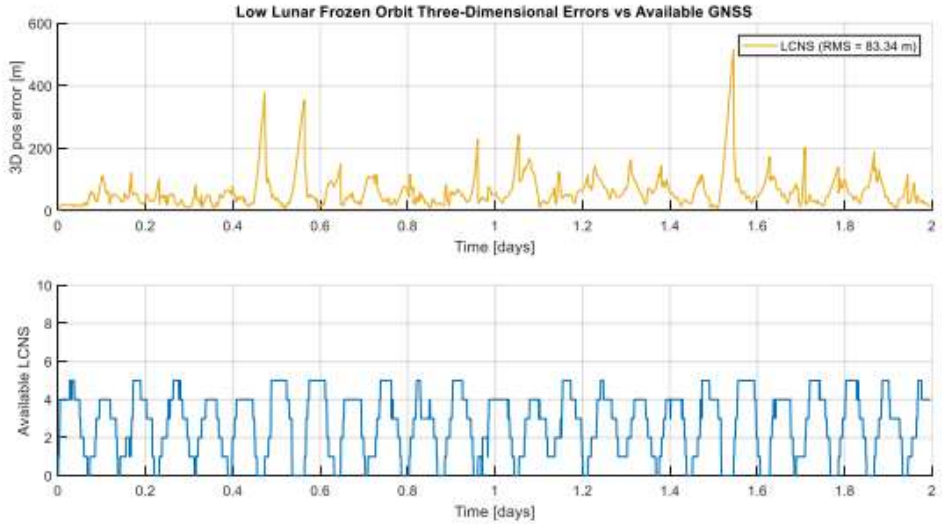

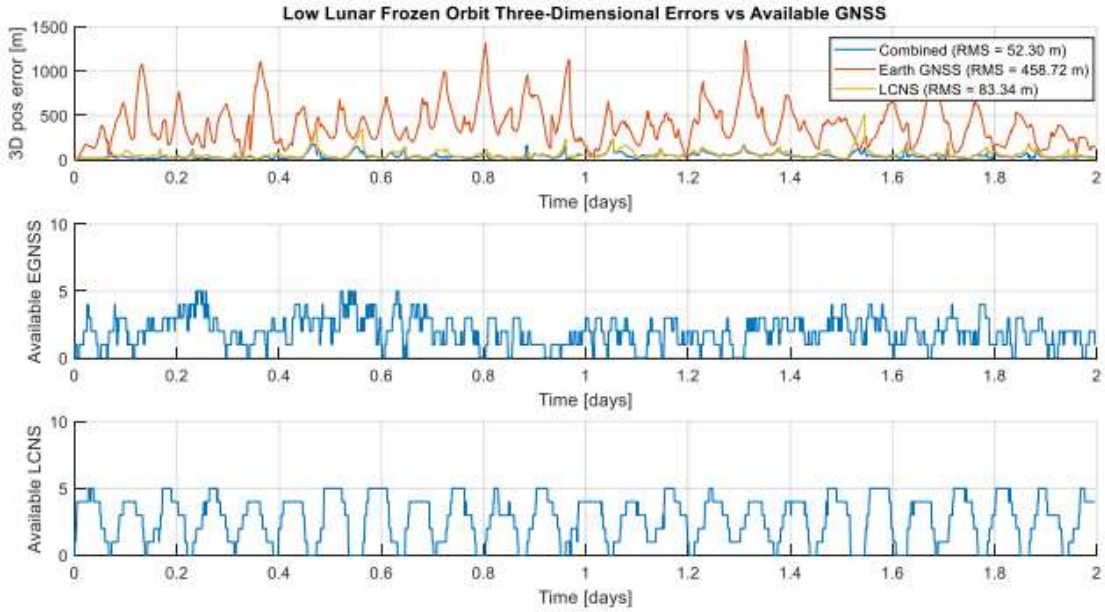

During the **occultation periods**, the **navigation error skyrockets**, as the filter is using exclusively the on-board dynamics model to update the state. Nevertheless, the error is acceptable, well contained within **500 meters**.

Conclusions

This study showed the navigation performance achievable by orbiting lunar spacecrafts, employing autonomous GNSS navigation for two different cases.

Using a **high-sensitivity GNSS receiver** and a dedicated **dynamic Extended Kalman Filter**, it was observed that satisfactory performance are achievable by using exclusively GNSS signal coming from Earth, especially for the Lunar Pathfinder scenario, whose orbit is further away from the Moon with respect to the LLFO.

The introduction of the **LCNS satellites** allowed to **improve navigation performance** in both cases. The improvement observed for the LLFO was significant: the combination of LCNS and Earth GNSS satellites improved RMS navigation error to around 50 m, against the 500 m observed when using Earth GNSS only.

References

[1] M. Mangialardo, M. M. Jurado, D. Hagan, P. Giordano, P. Zoccarato and J. Ventura-Traveset, "Autonomous Navigation For Moon Missions: A Realistic Performance Assessment, Considering Earth GNSS Signals And LCNS Constellation," 2022 10th Workshop on Satellite Navigation Technology (NAVITEC), 2022, pp. 1-11, doi: 10.1109/NAVITEC53682.2022.9847542.

[2] P. Giordano, A. Grenier, P. Zoccarato, L. Bucci, A. Cropp, R. Swinden, D. Gomez Ortero, W. El-Dali, W. Carey, L. Duvet, B. Hufenbach, F. Joly and J. Ventura-Traveset, "Moonlight navigation service - how to land on peaks of eternal light," IAC 2021 Congress Proceedings, 72nd International Astronautical Congress. https://dl.iafastro.directory/event/IAC2021/paper/64096/

[3] A. Grenier, P. Giordano, L. Bucci, A. Cropp, P. Zpccarato, R. Swinden, J. Ventura-Traveset, "Positioning and velocity performance levels for a Lunar Lander using a dedicated Lunar Communication and Navigation System," Navig. (Journal Inst. Navig. - Submitt. PEER Rev

[4] J. E. Donaldson, J. J. K. Parker, M. C. Moreau, D. E. Highsmith, and P. D. Martzen, "Characterization of on-orbit GPS transmit antenna patterns for space users," Navig. J. Inst. Navig., vol. 67, no. 2, pp. 411–438, 2020, doi: 10.1002/navi.361.

[5] V. Capuano, C. Botteron, J. Leclère, J. Tian, Y. Wang, and P. A. Farine, "Feasibility study of GNSS as navigation system to reach the Moon," Acta Astronaut., vol. 116, pp. 186–201, Nov. 2015, doi: 10.1016/J.ACTAASTRO.2015.06.007.

[6] V. Capuano, P. Blunt, C. Botteron, J. Leclère, J. Tian, Y. Wang, F. Basile and P. A. Farine , "Standalone GPS l1 C/A receiver for lunar missions," Sensors (Switzerland), vol. 16, no. 3, pp. 347– 368, 2016, doi: 10.3390/s16030347.

[7] P. Giordano, A. Grenier, P. Zoccarato, R. Swinden, D. Trenta, E. Shoenemann, F. Lucci, W. Enderle, B. Hufenbach, J. VenturaTraveset., "Orbit determination and time synchronisation in lunar orbit with GNSS – Lunar Pathfinder experiment," IAC 2021 Congress Proceedings, 72nd International Astronautical Congress. https://dl.iafastro.directory/event/IAC2021/paper/64095/

[8] "Moonlight: connecting Earth with the Moon." https://www.esa.int/ESA_Multimedia/Videos/2020/11/Moonlight_connecting_Earth_with_the_Moon/(lang)

References

[9] A. Grenier, P. Giordano, L. Bucci, A. Cropp, P. Zpccarato, R. Swinden, J. Ventura-Traveset, “Positioning and velocity performance levels for a Lunar Lander using a dedicated Lunar Communication and Navigation System,” Navig. (Journal Inst. Navig. - Submitt. PEER Rev.

[10] W. Zheng, Y. Huang, Z. Chen, G. Wang, Q. Liu, F. Tong, P. Li, L. Tong and F. Shu ., “Real-time and high accuracy VLBI in the CE-3 mission,” in International VLBI Service for Geodesy and Astrometry, 2014, pp. 466–472, Bibcode: 2014ivs..conf..466Z .

[11] S. Qin, Y. Huang, P. Li, Q. Shan, M. Fan, X. Hu and G. Wang, “Orbit and tracking data evaluation of Chang’E-4 relay satellite,” Adv. Sp. Res., vol. 64, no. 4, pp. 836–846, 2019, doi: 10.1016/j.asr.2019.05.028

[12] E. Mazarico, G. A. Neumann, M. K. Barker, S. Goossens, D. E. Smith, and M. T. Zuber, “Orbit determination of the Lunar Reconnaissance Orbiter: Status after seven years,” Planet. Space Sci., vol. 162, pp. 2–19, 2018, doi: 10.1016/j.pss.2017.10.004.

[13] A. Delépaut, P. Giordano and J. Ventura-Traveset , “Use of GNSS for lunar missions and plans for lunar in-orbit development,” Adv. Sp. Res., vol. 66, no. 12, pp. 2739–2756, Dec. 2020, doi: 10.1016/J.ASR.2020.05.018.

[14] M. Mangialardo, M. M. Jurado, D. Hagan, P. Giordano, and J. Ventura-Traveset, “The full Potential of an autonomous GNSS signal based navigation system for Moon missions,” in Proceedings of the 34th International Technical Meeting of the Satellite Division of The Institute of Navigation (ION GNSS+ 2021), 2021, pp. 1039–1052, doi: 10.33012/2021.18040.

[15] J. S. Parker, J. Smith, A. Forsman, C. Rabotin, C. Cain, and B. Cheetham, “The cislunar autonomous positioning system, CAPS,” Adv. Astronaut. Sci., vol. 169, pp. 573–583, 2019.

[16] M. Schönfeldt, A. Grenier, A. Delépaut, P. Giordano, R. Swinden and J. Ventura-Traveset, “Across the lunar landscape exploration with GNSS technology,” Insid. GNSS, vol. 2020, no. Oct, pp. 32– 37, 2020, URL in elib: https://elib.dlr.de/139404

References

[17] ESA, “ESA - Galileo will help Lunar Pathfinder navigate around Moon,” 2021, [Online]. Available: https://www.esa.int/Applications/Navigation/Galileo_will_help_ Lunar_Pathfinder_navigate_around_Moon.

[18] “Ephemeris.” https://ssd.jpl.nasa.gov/ephem.html.

[19] C. Zucca and P. Tavella, “A mathematical model for the atomic clock error in case of jumps,” Metrologia, vol. 52, no. 4, pp. 514– 521, 2015, doi: 10.1088/0026-1394/52/4/514.

[20]] https://www.quartzpro.com/tcxofacts.html.

[21] P. Steigenberger, S. Thoelert, and O. Montenbruck, “GPS III Vespucci: Results of half a year in orbit,” Adv. Sp. Res., vol. 66, no. 12, pp. 2773–2785, Dec. 2020, doi: 10.1016/J.ASR.2020.03.026

[22] M. Manzano-Jurado, J. Alegre-Rubio, A. Pellacani, G. SecoGranados, .J. López-Salcedo, E. Guerrero and A. García Rodríguez, “Use of weak GNSS signals in a mission to the moon,” 2014 7th ESA Work. Satell. Navig. Technol. Eur. Work. GNSS Signals Signal Process. NAVITEC 2014 - Proc., 2015, doi: 10.1109/NAVITEC.2014.7045151.

[23] P. Kwan, “IS-GPS-200 NAVSTAR GPS Space segment/navigation user segment interfaces, El Segundo, California: GPS Directorate - Space & Missile Systems Center (SMC) – LAAFB, 2019.”

[24] M. Anghileri, M. Paonni, D. Fontaneila, and B. Eissfeller, “GNSS data message performance: A new methodology for its understanding and ideas for its improvement,” Inst. Navig. Int. Tech. Meet. 2013, ITM 2013, pp. 638–650, 2013.

[25] D. Simon, “Optimal state estimation: Kalman, H∞, and nonlinear approaches,” Optim. State Estim. Kalman, H∞, Nonlinear Approaches, pp. 1–526, 2006, doi: 10.1002/0470045345.